Development 130, 929-940

doi:10.1242/dev.00308

Zebrafish *foxi1* mediates otic placode formation and jaw development

Keely S. Solomon[1,*], Tetsuhiro Kudoh[2,*,†], Igor B. Dawid[2] and Andreas Fritz[1,§]

[1]Department of Biology, Emory University, Atlanta, GA 30322, USA
[2]Laboratory of Molecular Genetics, National Institute of Child Health and Human Development, National Institutes of Health, Bethesda, MD 20892, USA
*These authors contributed equally to this work
[†]Present address: Department of Anatomy and Developmental Biology, University College London, Gower Street, London WC1E 6BT, UK
[§]Author for correspondence (e-mail: afrtiz@biology.emory.edu)

Accepted 18 November 2002

SUMMARY

The otic placode is a transient embryonic structure that gives rise to the inner ear. Although inductive signals for otic placode formation have been characterized, less is known about the molecules that respond to these signals within otic primordia. Here, we identify a mutation in zebrafish, *hearsay,* which disrupts the initiation of placode formation. We show that *hearsay* disrupts *foxi1,* a forkhead domain-containing gene, which is expressed in otic precursor cells before placodes become visible; *foxi1* appears to be the earliest marker known for the otic anlage. We provide evidence that *foxi1* regulates expression of *pax8,* indicating a very early role for this gene in placode formation. In addition, *foxi1* is expressed in the developing branchial arches, and jaw formation is disrupted in *hearsay* mutant embryos.

Key words: Foxi1, Forkhead, Zebrafish, Otic Placode, Ear, Jaw

INTRODUCTION

The vertebrate inner ear develops from the otic placode, a thickening of embryonic ectoderm that becomes morphologically visible around mid-somitogenesis in most vertebrate species (Baker and Bronner-Fraser, 2001; Torres and Giraldez, 1998). The otic placode is a transient structure, giving rise to the otic vesicle, which then proliferates and differentiates to form specialized cell types necessary for hearing and balance. Transplantation experiments in chick (Waddington, 1937) and amphibians (Jacobson, 1966; Yntema, 1933; Yntema, 1950) have shown that competence to form an otic placode is initially broadly distributed throughout the ectoderm that lies laterally to the neural plate. This region of competence becomes increasingly restricted as an ongoing response to multiple, overlapping signals emanating from surrounding tissues (Jacobson, 1963). Analyses of mutants that disrupt development of the hindbrain (Chisaka et al., 1992; Cordes and Barsh, 1994; Epstein et al., 1991; Lufkin et al., 1991; Moens et al., 1998), paraxial cephalic mesoderm and prechordal plate (Mendonsa and Riley, 1999) have demonstrated an inductive, partially redundant role for these tissues in the process of otic placode formation.

Recent work in chick and zebrafish has identified several of the signaling molecules that function in the earliest inductive steps. Chick *FGF19* and *FGF3* are expressed adjacent to the otic anlagen in the paraxial cephalic mesoderm and later in the hindbrain, and *FGF3* is additionally expressed in the otic placode and vesicle (Ladher et al., 2000; Mahmood et al., 1995). *FGF19* induces *Wnt-8c* expression in the neural tissue, and together these two signals can induce expression of otic markers (Ladher et al., 2000). In addition, misexpression of *FGF3* induces ectopic otic vesicle formation (Vendrell et al., 2000), and depletion of this molecule in explants of otic precursor tissue results in failure to form otic vesicles (Represa et al., 1991). During gastrulation, zebrafish *fgf3* and *fgf8* are expressed in mesendoderm and the presumptive hindbrain (Phillips et al., 2001). Loss of function of these two partially redundant genes leads to a severe reduction in otic vesicle size and a loss of *pax8* expression in the otic anlagen (Phillips et al., 2001); *pax8* is the earliest known marker of otic precursor cells in both fish and mammals (Pfeffer et al., 1998). Thus, these and other experiments (Kozlowski et al., 1997; Woo and Fraser, 1997) show that induction of the otic placode begins as early as mid-gastrulation and that Fgf-signaling molecules provide some of the earliest inductive signals in this process.

Less is known about early acting genes that function within the otic precursor cells to respond to inductive signals and elicit placode formation. No otic defect has been reported for a knockout of mouse *Pax8* (Mansouri et al., 1998), and otic function of zebrafish *pax8* has not been characterized. Zebrafish *dlx3b* and *dlx4b* (formerly *dlx3* and *dlx7,* respectively), two members of the *Distal-less* family of transcription factors, are expressed shortly after the onset of *pax8* expression in presumptive otic tissue (Akimenko et al., 1994; Ekker et al., 1992; Ellies et al., 1997). Embryos homozygous for a deletion of these genes lack otic placodes, and morpholino-mediated knockdown of one or both genes demonstrates their partially redundant function in otic placode development (Solomon and Fritz, 2002). In mouse, targeted disruption of the *Drosophila eyes absent* homologue *Eya1*

leads to a severe defect, as development arrests at the otic vesicle stage and the otic vesicle regresses by apoptosis; however, early placode induction occurs normally in these embryos (Xu et al., 1999).

We have identified a mutation in zebrafish, *hearsay* (*hsy*), which disrupts the *foxi1* gene and results in a reduction or loss of the otic placode and vesicle. Foxi1 is a member of the forkhead family of winged-helix transcription factors that share a highly conserved, 110 amino acid DNA-binding domain (Kaufmann and Knochel, 1996). Founding forkhead family members, *Drosophilia* Forkhead (Weigel et al., 1989) and mammalian HNF-3α (Lai et al., 1990), have been shown to function in the development of terminal structures in the embryo and in regulation of liver gene expression, respectively. Currently, more than 100 forkhead genes have been identified in species ranging from yeast to humans (see the Winged Helix Proteins site; http://www.biology.pomona.edu/fox.html). These genes have been implicated in a broad range of biological functions, including early patterning and morphogenesis (Pogoda et al., 2000), cell specification (Miller et al., 1993), gene regulation in differentiated tissues (Clevidence et al., 1994), cell proliferation (Dou et al., 1999) and tumorigenesis (Kops and Burgering, 1999). So far, few forkhead genes have been implicated specifically in otic development. Of the more than a dozen forkhead genes identified in zebrafish (Biggs and Cavenee, 2001; Boggetti et al., 2000; Dirksen and Jamrich, 1995; Odenthal and Nusslein-Volhard, 1998; Strahle et al., 1993; Topczewska et al., 2001), only one, *foxg1* (formerly *zBF-1*), is expressed in the otic vesicle (Toresson et al., 1998), and no otic defect is reported in mice that are homozygous null for the *BF-1* gene (Xuan et al., 1995). In mouse, *Foxf2* is expressed in the otic vesicle, as well as other tissues (Aitola et al., 2000), but no functional analysis has been reported for this gene. *Foxi1* is expressed in the otic vesicle, and mice homozygous for a targeted inactivation of this gene have severely malformed inner ears and exhibit both cochlear and vestibular dysfunction (Hulander et al., 1998).

Here we report the functional characterization of the *hsy/foxi1* gene in zebrafish. Embryos homozygous for the *hsy* mutation display a severe reduction or loss of the otic placode, providing the first example of a single gene mutation that can lead to a complete loss of otic placodes. In addition, *hsy* mutant embryos also exhibit a malformation of the jaw. Expression analysis of *foxi1* suggests a direct role for this gene in the development of the otic placode and branchial arch derivatives. We demonstrate that otic expression of *pax8* is absent in *hsy* mutants, and that misexpression of *foxi1* can induce ectopic *pax8* expression. Together, these data suggest that *foxi1* function is required within otic precursor cells for the earliest stages of otic placode induction.

MATERIALS AND METHODS

Strains

Zebrafish (*Danio rerio*) were raised and maintained according to standard procedure (Westerfield, 2000). The *hearsay* mutation was identified through random intercrosses among a partially inbred line of store-bought fish. Embryos were raised at 28.5°C and staged as described (Kimmel et al., 1995).

Cloning and construction of expression plasmid

A partial zebrafish *foxi1* clone was identified in an expression pattern screen using high-throughput in situ hybridization (clone 3015) (Kudoh et al., 2001). The 5′ end of *foxi1* was subsequently generated by 5′-RACE using the SMART RACE Kit (Clontech) with a gene-specific primer (5′-cgtctctgcttcggaccgcgtttcc-3′), and sequenced. Full-length cDNA was then amplified and subcloned into the expression vector pCS2+.

Whole-mount in situ hybridization

Whole-mount in situ hybridization was performed as described (Thisse and Thisse, 1998), and double labeling as outlined (Itoh et al., 2002; Jowett, 2001). Embryos were prepared for sectioning as described (Westerfield, 2000), and 5 μm plastic sections or 15 μm frozen sections were generated. The zebrafish *dlx3b* (Ekker et al., 1992), *dlx4b* (Ellies et al., 1997), *dlx5a* (Akimenko et al., 1994), *dlx2a* (Akimenko et al., 1994), *pax8* (Pfeffer et al., 1998), *pax2a* (Krauss et al., 1991), *krox20* (Oxtoby and Jowett, 1993), *crestin* (Luo et al., 2001; Rubinstein et al., 2000) and *otx2* (Li et al., 1994) probes were previously described.

Morpholino injections

Morpholino antisense oligonucleotides (Gene Tools, LLC, Corvallis, OR) were as follows (complementary bases to the predicted start codon are indicated in italics): *foxi1*, 5′-TAATCCGCTCTCCCT-CCAGAAA*CAT*-3′; Gene Tools, LLC standard control oligo (http://www.gene-tools.com/).

Alcian Green staining

Embryos were fixed overnight in 4% paraformaldehyde, followed by several washes in PBT (phosphate-buffered solution +0.1% Tween 20) the next day. The embryos were then placed in 30% hydrogen peroxide for approximately 20 minutes to bleach pigment cells, washed in PBT several more times, then stained in 0.37% HCl/70% ethanol solution/0.1% Alcian Green for 1.5 hours. This was followed by several brief washes in 1%HCl/70% ethanol. The tissues were cleared in 50% glycerol/0.5% KOH and the cartilages were photographed.

Genotyping

DNA was prepared after in situ hybridization from embryos sorted by phenotype, and a 607 bp PCR fragment was amplified with the following primers: F, 5′-AAACCCCTCAGAGACGAGCACA-CTCA-3′; R, 5′-CTGCCAGCCGGCTTTACTTTTCTTGT-3′. The amplification products were digested with *Taq*I, which only cuts the mutant sequence, and analyzed on a 1.5% agarose gel.

RESULTS

Isolation and morphological characterization of *hearsay*

The *hsy* mutation was identified in a screen for mutations affecting early ear development in zebrafish embryos. At 24 hours post-fertilization (24 hpf), wild-type embryos display easily discernable otic vesicles that have cavitated to form lumens, each containing two otoliths (Fig. 1A). The vesicles are larger but retain a similar structure at two days post-fertilization (2d) (Fig. 1I). In contrast, homozygous *hsy* embryos display small or no otic placodes and vesicles (Fig. 1B). This defect is visible by the 14-somite stage and persists through the remainder of the embryogenesis and larval stages. The *hsy* phenotype is variable in that some mutants lack otic vesicles entirely (Fig. 1F), whereas others develop a small lumen with no or one otolith (Fig. 1K,L). A fraction of embryos

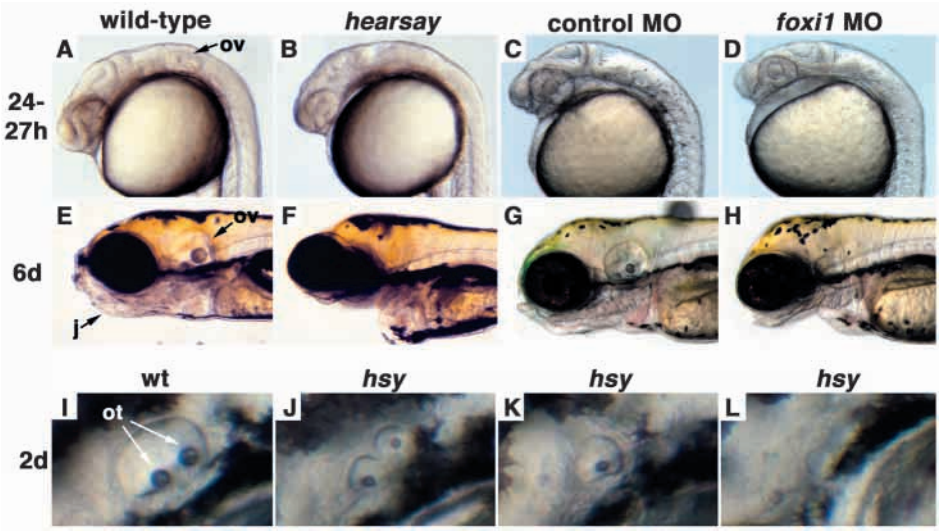

Fig. 1. *hearsay* mutant embryos display defects in otic and jaw development. All panels show lateral views of live embryos with anterior to the left. (A) Wild-type and (B) *hsy* embryos at 24 hpf. (C,D) Twenty-seven hpf wild-type embryos injected with (C) control morpholino and (D) *foxi1* morpholino. (E-H) Six-day-old embryos: (E) wild type, (F) *hsy*, (G) wild type injected with control morpholino and (H) wild type injected with *foxi1* morpholino. (I-L) Otic vesicles in (I) wild-type and (J-L) *hsy* mutant embryos at 2 days. j, jaw; ot, otolith; ov, otic vesicle.

have two small lumens that each contains a single otolith (Fig. 1J), a phenotype reminiscent of *quadro* mutants (Malicki et al., 1996), although no complementation tests between the two mutations have been performed. In addition to this otic defect, *hsy* mutants exhibit a defect in jaw development that becomes apparent by four days post-fertilization (4d). In 6d wild-type embryos, most of the cartilaginous elements of the jaw have begun to develop and the mouth appears to protrude from the anterior-most region of the head (Fig. 1E), whereas *hsy* mutant jaws are much smaller than in wild type and the protruding mouth is not visible (Fig. 1F). The *hsy* phenotype is recessive and fully penetrant; approximately 25% of embryos from a cross between *hsy* carriers exhibit some degree of otic and jaw defects, whereas the remaining 75% appear normal. The *hsy* mutation is lethal; mutant larvae fail to inflate the swimbladder and die at around 7-8d.

The *hearsay* mutation disrupts the *foxi1* gene

To identify the gene disrupted by the *hsy* mutation, DNA was prepared from individual mutant and wild-type embryos and tested for linkage to polymorphic microsatellite markers (http://zebrafish.mgh.harvard.edu) (Shimoda et al., 1999). The mutation was localized to LG12, between markers Z14982 (two recombinants/265 chromosomes tested) and Z8344 (two recombinants/253 chromosomes tested, data not shown).

One candidate gene in this region, *3015*, was identified as part of a screen for expression patterns of embryonic cDNAs (Kudoh et al., 2001). Clone *3015* was localized by radiation hybrid (RH) mapping (LN54 panel) (Hukriede et al., 2001; Hukriede et al., 1999) on LG12 in the vicinity of the *hsy* map position; we will provide evidence below that the *hsy* locus encodes the *3015* sequence. A BLAST search of the NCBI database with the *3015* sequence identified it as encoding a forkhead domain-containing protein. This sequence was classified in the Fox I class and consequently named *foxi1* (see the Winged Helix Proteins site; http://www.biology.pomona.edu/fox.html) (Fig. 2A). The zebrafish Foxi1 protein shares 52% identity with *Xenopus* FoxI1c and 40% with human FOXI1; the forkhead domains are 95% and 94% identical, respectively.

To test whether *foxi1* is disrupted by the *hsy* mutation, we amplified and sequenced fragments representing the gene from individual haploid mutant and wild-type embryos. Mutant embryo DNA contained a two base-pair deletion close to the amino-terminus of the protein, creating a shift in the reading frame in codon 41 (Fig. 2B). The shifted sequence continues for an additional 117 amino acids with no similarity to known proteins. Thus, the mutation eliminates most of the wild-type Foxi1 protein including the forkhead domain, and most likely represents a null mutation. No additional differences were found between mutant and wild-type sequences. The two base-pair deletion in *hsy* creates a *Taq*I restriction site, and we used this polymorphism to test for linkage of the mutant phenotype to this sequence change. Genomic DNA was isolated from individual embryos generated from crosses of *hsy* heterozygous parents, amplified and tested for the *TaqI* polymorphism: no recombinants between the *hsy* mutation and the *TaqI* polymorphism were found in more than 450 meioses tested. Conversely, no homozygotes for the *TaqI* polymorphism were found in 700 wild-type siblings. Thus, the *hsy* mutation is tightly linked to the two-base deletion, providing direct genetic evidence for the conclusion that *hsy* disrupts *foxi1*.

To test whether inhibition of *foxi1* translation could phenocopy the *hsy* mutation, we injected wild-type embryos with a morpholino antisense oligonucleotide (Nasevicius and Ekker, 2000) against *foxi1* mRNA. Injection of this morpholino produced a phenotype almost identical to that of *hsy*; otic vesicles of injected embryos were very small or absent (Fig. 1D), and jaws were reduced in size (Fig. 1H). These injected embryos displayed variability in severity of the otic defect, similar to the variability seen in the mutants. None of these phenotypes were observed in embryos injected with a control morpholino (Fig. 1C,G). This observation confirms the conclusion, based on our linkage and sequencing data, that the *hsy* phenotype is caused by disruption of the *foxi1* gene.

foxi1 expression

The expression profile of *foxi1* is shown in Fig. 3. At 50% epiboly, the earliest stage examined, *foxi1* is expressed in a portion of the ectoderm (Fig. 3A), and this domain of expression becomes broader and stronger by 75% epiboly (Fig. 3B). To determine whether *foxi1* is expressed in neural or non-

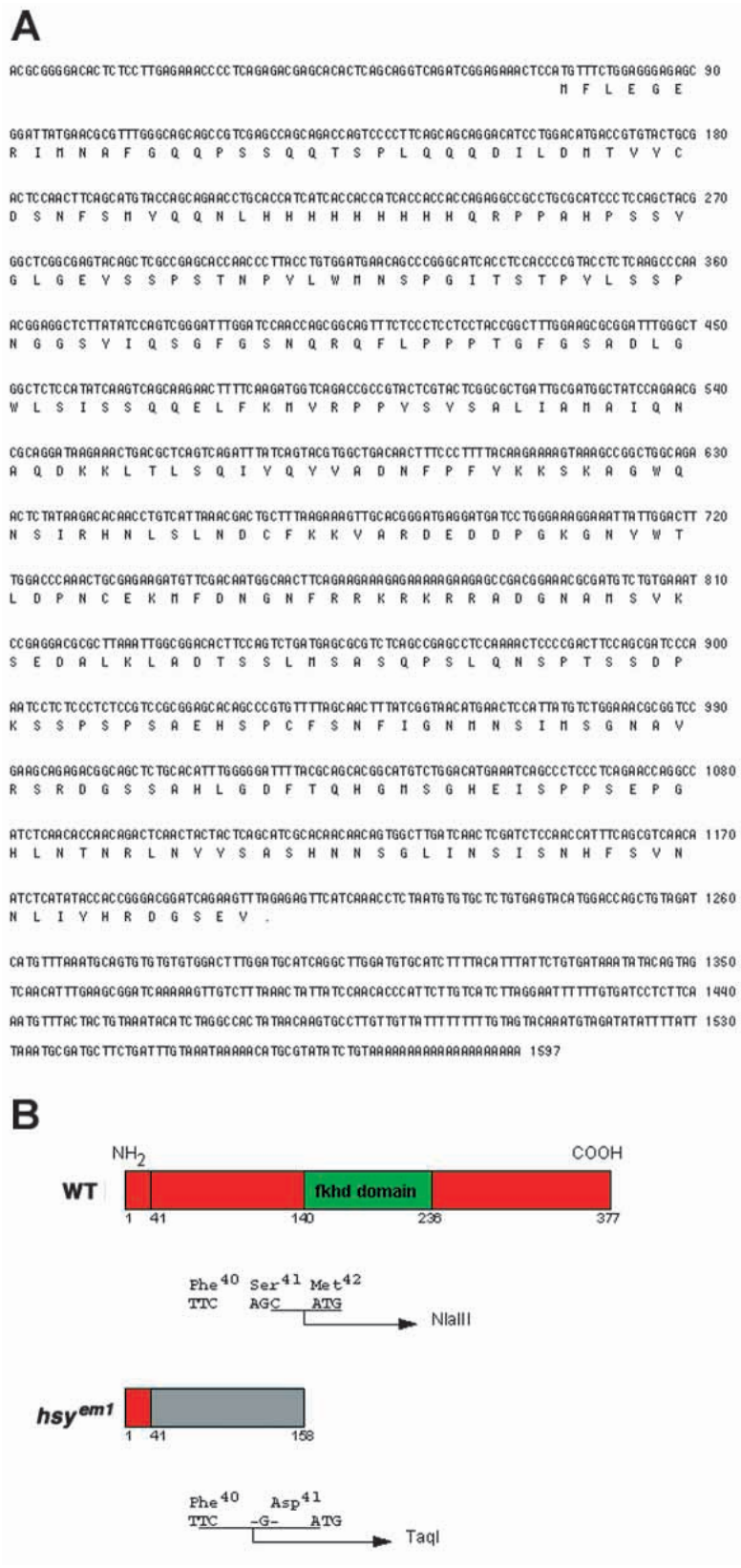

Fig. 2. The *hsy* phenotype is caused by a disruption of *foxi1*. (A) Nucleotide sequence and predicted ORF of zebrafish *foxi1*(GenBank Accession Number, AY204207). (B) Schematic of Foxi1 protein in wild type and *hsy*. A two-base deletion produces a frameshift in codon 41 and results in a truncated protein of 158 amino acids.

neural ectoderm, double in situ labeling was performed with *otx2*, a marker of neural ectoderm (Li et al., 1994). *foxi1* expression does not overlap with *otx2*, indicating that it is expressed in non-neural ectoderm (Fig. 3C).

By the beginning of somitogenesis, *foxi1* expression has become confined to two domains that lie laterally to the neural plate in the dorsal ectoderm (Fig. 3D-F), whereas expression is no longer detectable in ventral ectoderm. Based on double in situ labeling with *otx2*, the anterior-most region of *foxi1* expression lies just posterior to the midbrain-hindbrain boundary (Fig. 3D,F). At the three-somite stage, the two domains of *foxi1* expression have become more compact, but are still located in approximately the same position lateral to the hindbrain (Fig. 3G,H). A transverse section of an embryo at this stage shows that the more lateral region of *foxi1* expression is confined to the upper, ectodermal layer of cells, whereas more medially, ectodermal and mesendodermal expression can be seen (Fig. 3I).

To determine whether *foxi1* is expressed in otic precursor cells, double labeling was performed with both *pax8* and *dlx3b* at the one-somite stage stage. The *foxi1* expression domain overlaps *pax8* otic expression at this stage, sharing approximately the same posterior and medial boundaries, but extending further than *pax8* in the anterior and lateral directions (Fig. 3J,K). *foxi1* expression also overlaps with *dlx3b* at the one-somite stage, although *dlx3b* expression is more extensive along the a-p axis. Within the region of overlap, *foxi1* and *dlx3b* share the same medial border, but *foxi1* extends further laterally (Fig. 3L). These results indicate that *foxi1* is expressed in otic precursor cells at late gastrula and early somitogenesis stages. At mid- and late-somitogenesis stages, *foxi1* expression is no longer detectable in the otic placode and vesicle, respectively (Fig. 4A-C and data not shown).

At the 18-somite stage, *foxi1* is expressed in throughout the pharyngeal arches (Fig. 4A,B), and expression in this region remains detectable at 28 hpf (Fig. 4C), the latest stage examined. Sections through the pharyngeal arches of 28 hpf embryos reveal that *foxi1* expression appears to extend into the pouches that separate the individual arches (Fig. 4D,E). *dlx2a* (formerly *dlx2*) is expressed in cranial neural crest cells that migrate to reside within the pharyngeal arch primordia by 16 hpf, and expression in the arches persists through the beginning of the second day of development (Akimenko et al., 1994). Sections through 26 hpf embryos double-labeled for expression of *dlx2a* (red) and *foxi1* (purple) show that most of the *dlx2a*-expressing presumptive neural crest cells do not express *foxi1* (Fig. 4F,G). Rather, *foxi1* expression partially surrounds these cells, consistent with the position of the pouches and/or clefts that separate the neural crest-containing arches. It is unclear whether any of the *foxi1*-expressing cells also express *dlx2a*, as the purple

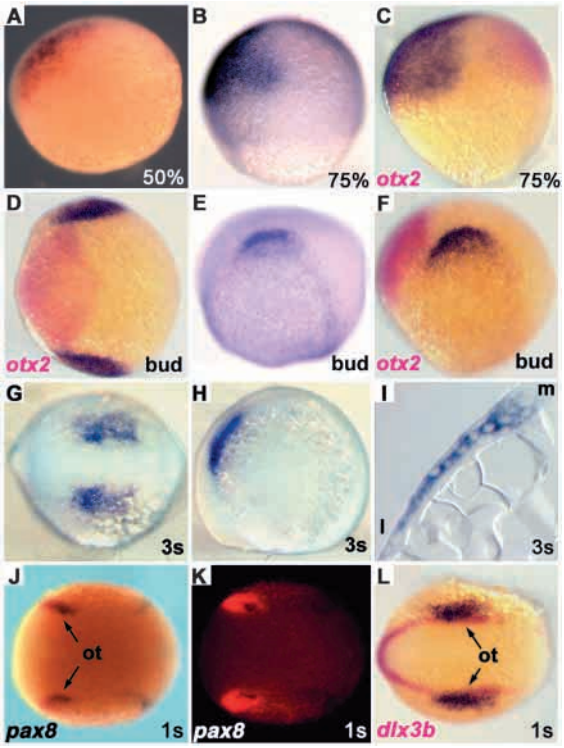

Fig. 3. *foxi1* expression. All panels show *foxi1* expression in dark purple, except J and K (red). Where double in situ labeling is shown, the second marker is indicated in the panel. Anterior is towards the left in D-H,J-O. (A) 50% epiboly and (B,C) 75% epiboly stages, animal pole towards the top, dorsal towards the right. (C) Double in situ labeling with *otx2* shown in red. (D-F) Bud stage embryos: (D) dorsal and (E,F) lateral views. (D,F) Double in situ labeling with *otx2* in red. (G,H) Three-somite stage embryo: (G) dorsal and (H) lateral views. (I) Transverse section of a three-somite stage embryo. (J-L) One-somite stage embryo: dorsal views. (J,K) Double labeling with *pax8* in dark purple, *foxi1* in red. (L) double labeling with *dlx3b* in red. l, lateral; m, medial; ot, otic primordia.

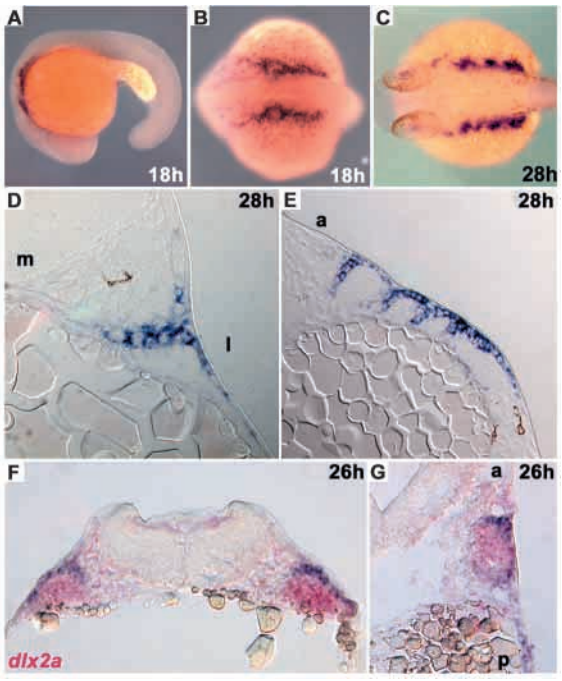

Fig. 4. *foxi1* pharyngeal arch expression. (A-C) *foxi1* expression in whole-mount embryos. (A) 18 hpf, lateral view; (B) 18 hpf, dorsal view; (C) 28 hpf, dorsal view. (D,E) *foxi1* expression in 5 μm sections through the pharyngeal arches of 28 hpf embryos. (D) Transverse section and (E) sagittal section. (F,G) 15 μm sections through pharyngeal arch region of 26 hpf embryos: *foxi1* expression shown in purple, *dlx2a* expression shown in red. Transverse (F) and sagittal (G) sections. a, anterior; l, lateral; m, medial; p, posterior.

substrate masks the expression of the red. Thus, *foxi1* is expressed predominantly in cells other than neural crest in the pharyngeal arches.

foxi1 function in otic placode specification

To study the timing of *foxi1* function in otic development, we examined the expression of several early otic markers in *hsy* mutant embryos. *pax8* expression is detectable in the presumptive otic domain of wild-type embryos as early as 90% epiboly, whereas *pax2a* is expressed in otic cell precursors beginning in early somitogenesis, several hours before otic placodes become visible (Krauss et al., 1991; Pfeffer et al., 1998). We find that both *pax8* and *pax2a* expression is completely absent in the otic domain of approximately one quarter of three- to five-somite stage embryos from a cross between *hsy* heterozygotes (Fig. 5A-D); these embryos are presumed to represent *hsy* homozygotes. In the embryos in which otic expression was absent, *pax8* and *pax2a* expression in the pronephros and *pax2a* expression in the midbrain-hindbrain boundary was comparable to wild type, providing a control for the in situ reaction.

dlx3b expression was also examined in three-somite stage embryos from a cross between *hsy* heterozygotes. At this stage, *dlx3b* is expressed in a continuous ectodermal stripe around the edge of the neural plate, and expression is upregulated in the otic and olfactory primordia (Akimenko et al., 1994; Ekker et al., 1992). We found that one-quarter of the embryos from this cross lack this upregulation in the otic region (Fig. 5E,F). To confirm that these embryos were mutants, we sorted them based on this phenotype and individually genotyped them for the *hsy* mutation (Fig. 5G). One-hundred per cent (9/9) of the embryos that lacked *dlx3b* otic upregulation were homozygous for the *hsy* mutation, and 100% (21/21) of those that had been judged as having normal expression were heterozygous or homozygous for the wild-type allele.

foxi1 induces ectopic *pax8* expression

To learn more about the function of *foxi1*, we injected an expression construct containing the full-length coding sequence under the control of the cyto megalo virus (CMV) promoter into one-cell stage wild-type embryos. *pax8* expression was examined in injected embryos fixed at three- to five-somite stage. We found, in addition to the normal domains of otic and pronephric expression, *pax8* was also expressed in many ectopic locations in the injected embryos (Fig. 6A). This ectopic expression was observed in 15/18 embryos injected with the expression construct, and in 16/18 embryos injected with in vitro transcribed *foxi1* RNA (not shown). Double in situ labeling with *foxi1* reveals that the ectopic domains of *pax8* expression coincide with ectopic *foxi1* expression (Fig. 6A,B).

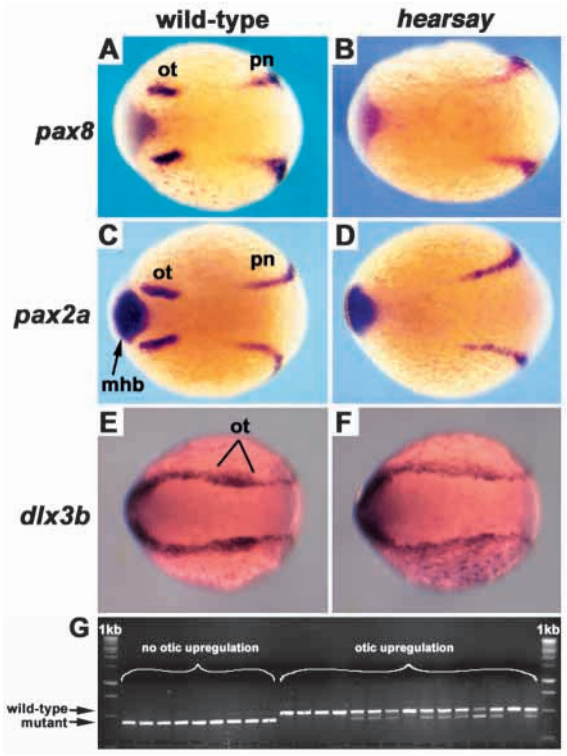

Fig. 5. Markers of early placode induction are absent in *hsy*. (A-F) In situ hybridizations with three- to five-somite stage embryos: dorsal views, anterior towards the left. (A,C,E) wild-type and (B,D,F) *hsy* embryos. (A,B) *pax8* expression, (C,D) *pax2a* expression and (E,F) *dlx3b* expression. (G) *TaqI* genotyping for *dlx3b* in situ. Migration position for *hsy* mutant and wild-type fragments are indicated at the left of the gel. mhb, midbrain-hindbrain boundary; ot, otic primordia; pn, pronephros.

This co-localization of ectopic expression was observed in 11/16 embryos injected with the *foxi1* expression construct. Ectopic expression of *dlx3b*, *dlx5a* (formerly *dlx4*) and *dlx4b*, but not *pax2a*, was also observed in these embryos (data not shown).

Expression of late otic markers in *hearsay* mutants

We examined the effect of the *hsy* mutation on later stages of otic development by in situ hybridization with *dlx3b*, *dlx4b* and *dlx5a*. These three genes are expressed in several developing cranial structures during mid-late somitogenesis, including the otic vesicle and the visceral arches (Akimenko et al., 1994; Ekker et al., 1992; Ellies et al., 1997). At 16-somite stage, *dlx4b* and *dlx3b* are expressed in the olfactory placode and the otic vesicle in wild-type embryos (Fig. 7A; *dlx3b* not shown), and this otic expression was reduced or absent in all *hsy* mutants examined (Fig. 7B; *dlx3b* not shown). In 24 hpf wild-type embryos, *dlx3b*, *dlx5a* and *dlx4b* are expressed in the olfactory placode, visceral arches and otic vesicle, and *dlx5a* is additionally expressed in several structures of the forebrain (Fig. 7C,E; *dlx4b* not shown). *hsy* mutants display a variable reduction or absence of otic staining for all of these genes at this stage (Fig. 7D,F,G; *dlx4b* not shown). Although all mutant embryos examined had reduced otic expression of these genes, the degree of reduction was variable, ranging from no otic expression to a reduction in size of the otic expression domain. This observation is in concordance with the variability in the otic phenotype observed by morphological inspection, as described above. In addition, we observe a loss of expression in the branchial arches in some of the mutant embryos, although this phenotype is not as penetrant as the reduction in otic expression (Fig. 7D for *dlx3b*, F and G for *dlx5a*; *dlx4b* not shown).

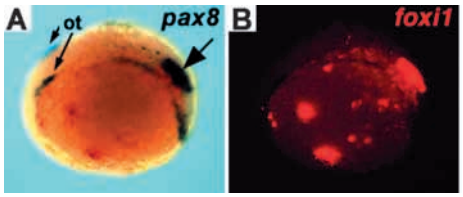

Fig. 6. Misexpression of *foxi1* can induce ectopic *pax8* expression. (A,B) Double in situ labeling of one-somite stage wild-type embryo injected with a *foxi1* expression vector. The same embryo is shown in both panels, dorsolateral view, anterior towards the left. (A) *pax8* expression shown in dark purple. The large arrow indicates an example of ectopic expression. (B) *foxi1* expression shown in red. ot, otic primordia.

Effects of *hearsay* in jaw formation

Alcian Green staining reveals that all of the major cartilaginous elements of the jaw are present in *hsy* mutants at 5 d (Fig. 8A,B). However, these elements are spaced more compactly in the a-p dimension, and this compression presumably results in the reduced jaw phenotype observed in the mutant.

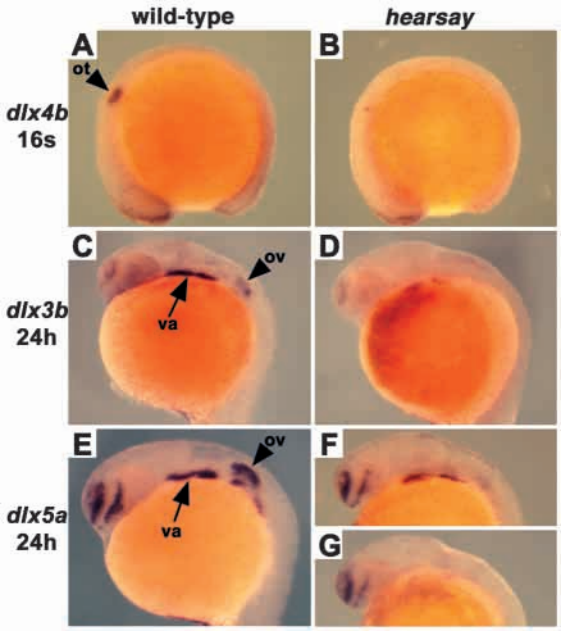

Fig. 7. Expression of markers for branchial arches and late-otic development is affected in *hsy*. RNA in situ hybridization with (A,C,E) wild-type and (B,D,F,G) *hsy* mutant embryos. (A,B) *dlx4b* expression, 16-somite stage. (C,D) *dlx3b* expression, 24 hpf. (E-G) *dlx5a* expression, 24 hpf. Note the loss of visceral arch expression in G. Forebrain and olfactory placode expression is unaffected in *hsy*. Lateral views, anterior towards the left in all panels. ot, otic placode; ov, otic vesicle; va, visceral arches.

Specifically, the first or mandibular arch derivatives, which include the mandibular and palatoquadrate elements, appear normal in *hsy* mutants. The second or hyoid arch derivatives appear to be differentially affected: whereas the basihyal element seems to form normally, the ceratohyal (ch) element is often in a more perpendicular position with respect to the a-p axis. In addition, the ch element is shorter and thicker than in wild-type larvae, and this thickening may in part be caused by a fusion with the first gill arch. The posterior or gill arch elements are derived from the third through seventh pharyngeal arches. Like the ch, the gill arches of *hsy* mutants often lie in a more perpendicular orientation with respect to the a-p axis, and they are shorter and more closely spaced.

The cartilage elements of the jaw are largely derived from cranial neural crest cells that migrate into the area of the branchial arches. *foxi1* is expressed in the region of the branchial arches (Fig. 4), providing a basis for its potential function in the formation of this tissue. In addition to the jaw, cranial neural crest contributes to pigmentation, the developing heart, the enteric nervous system (ENS) and the sensory portion of cranial ganglia. We have not been able to detect any defects in pigmentation or heart morphology, and anti-Hu staining revealed no ENS defects (data not shown). Cranial ganglia were not examined. To address the possible effect of the *hsy* mutation on the migration and differentiation of neural crest within the branchial arches, we examined expression of *crestin*, a marker for neural crest cells (Luo et al., 2001; Rubinstein et al., 2000). All of the major domains of *crestin* expression were present in *hsy* mutants, including the mandibular, hyoid and vagal cranial crest streams (Fig. 8C,D). However, double in situ labeling with *krox20*, which marks rhombomeres 3 and 5 (r3 and r5), reveals that the hyoid and vagal *crestin* domains are more closely spaced in mutant embryos (Fig. 8C,D). In particular, the vagal crest domain extends past the anterior boundary of the *krox20* r5 stripe in *hsy* mutants, ending in a region adjacent to r4 (Fig. 8D), whereas in wild-type embryos, the anterior boundary of this expression domain lies laterally to the middle of the *krox20* r5 stripe (Fig. 8C). This observation may provide an explanation for the fusion of the ch element (hyoid crest derivative) and the third gill arch (vagal crest derivative) seen in *hsy* mutant larvae.

dlx2a expression in the cranial neural crest also appears to be affected in *hsy* mutant embryos at the 18-somite stage (Akimenko et al., 1994; Ellies et al., 1997) (Fig. 8E,F). First, similar to *crestin*, the three domains of expression in the cranial crest are more closely spaced. Second, we consistently observe an increase in intensity of *dlx2a* staining in the mutants. Likewise, the expression of *foxi1* itself is more intense in *hsy* mutant embryos (Fig. 8G,H). This conclusion was supported by genotype analysis. All the embryos derived from a cross between *hsy* heterozygotes were hybridized in situ with *dlx2a* or *foxi1*, sorted by 'increased' or 'normal' expression of the examined marker, and genotyped for the *hsy* mutation using the *Taq*I restriction polymorphism (see Fig. 2B). For *foxi1* expression at the 18-somite stage, genotyping revealed that 100% (11/11) of increased expression embryos were homozygous mutant, and 100% (32/32) of normal expression embryos were heterozygous or homozygous wild type (Fig. 8I). For *dlx2a* at the 18-somite stage, 86% (12/14) of increased expression embryos were mutant and 100% (32/32) of normal expression embryos were heterozygous or wild type. Using 24 hpf embryos we found that, for *foxi1*, 81% (13/16) of increased embryos were mutant and 91% (51/56) of normal embryos were wild type, and for *dlx2a*, 100% (19/19) increased embryos were mutant and 100% (33/33) of normal embryos were wild type. Thus, increased expression of *dlx2a* and *foxi1* in the branchial arches is a consequence of the *hsy* mutation. No increase in expression of *foxi1* was detectable during gastrulation or early somitogenesis (data not shown). This increased expression of *foxi1* in *hsy* mutant embryos is suggestive of a function for *foxi1* as a negative transcriptional regulator. However, it remains unclear whether this

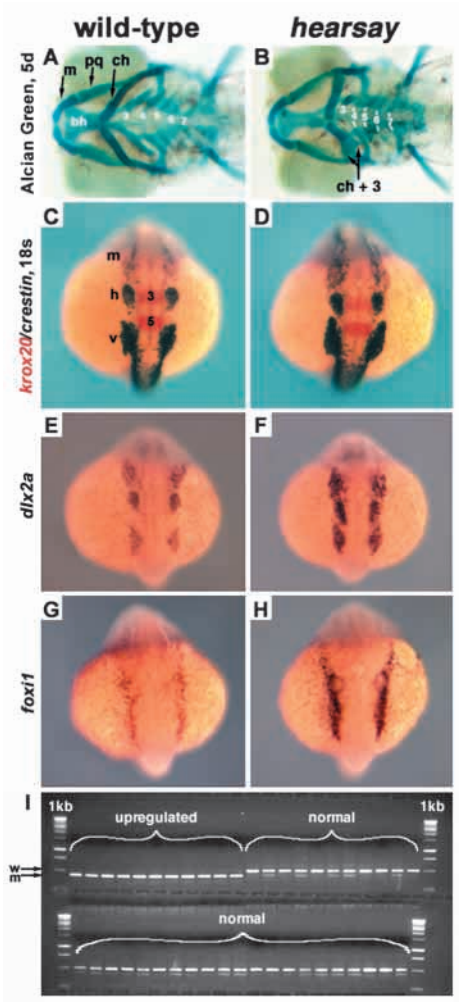

Fig. 8. Analysis of jaw and neural crest in *hsy*. (A,C,E,G) Wild-type and (B,D,F,H) *hsy* mutant embryos. (A,B) Alcian Green staining of cartilaginous jaw elements at 5 days. Ventral views, anterior towards the left. Cartilages: bh, basihyal; ch, ceratohyal; m, mandibular; pq, palatoquadrate; 3-7, gill cartilages derived from branchial arches P3-P7. m and pq are P1 derivatives; ch and bh are derived from P2. ch+3 indicates unilateral fusion of ceratohyal with gill arch 3 in mutant. (C-H) Expression analysis at the 18-somite stage: dorsal views, anterior towards the top. (C,D) Double labeling with *crestin* (dark purple) and *krox 20* (red). (E,F) *dlx2a* expression. (G,H) *foxi1* expression. (I) *Taq*I restriction polymorphism genotyping data for *foxi1* in situ hybridization at the 18-somite stage, sorted as either 'upregulated' or 'normal expression'. m, mandibular neural crest (nc) stream; h, hyoid nc; v, vagal nc; 3 and 5, *krox20* expression in rhombomeres 3 and 5.

autoregulation is direct or indirect and whether the increased expression of *foxi1* or *dlx2a* is caused by an increase in the number of cells expressing these genes or elevated expression levels.

DISCUSSION

The role of *foxi1* in otic placode formation

Although several inductive signals for otic placode formation have been characterized, including chick FGF2 and FGF8 (Adamska et al., 2001), FGF3 (Mahmood et al., 1995; Vendrell et al., 2000), FGF19 and Wnt8c (Ladher et al., 2000), and zebrafish fgf3 and fgf8 (Phillips et al., 2001), little is known about the genes that respond to these signals within the pre-placodal tissue and initiate the program of otic development. One gene that might participate in this inductive response is *pax8*, which, previous to this study, was the earliest gene reported to be expressed in otic precursor tissue (Pfeffer et al., 1998). However, no otic defects were observed in mice homozygous for a targeted inactivation of *Pax8* (Mansouri et al., 1998), and no mutations in this gene have been described in zebrafish. *dlx3b* and *dlx4b* are also expressed in the otic primordia, shortly after the onset of *pax8* expression, and are additionally expressed in the olfactory primordia (Akimenko et al., 1994; Ekker et al., 1992; Ellies et al., 1997). Embryos homozygous for *b380*, a deletion for both of these genes, fail to form otic and olfactory placodes, revealing an early role for *dlx3b* and *dlx4b* in placode induction (Solomon and Fritz, 2002). Although *pax2a*, a slightly later otic marker than *pax8*, fails to be expressed in the otic precursor domain of these embryos, the transient expression of *pax8* in otic primordia is normal, indicating that early otic characteristics are induced in *b380* mutant embryos.

In this work we have identified a mutation, *hearsay*, which leads to a severe reduction or loss of the otic placode in zebrafish. Further, we show that the *hsy* phenotype is caused by a disruption of *foxi1*, which was identified in a screen for genes that are differentially expressed during zebrafish embryogenesis (Kudoh et al., 2001). Double in situ labeling with known otic markers shows that *foxi1* is expressed very early in otic precursor cells, as early or earlier than *pax8*. Loss of *pax8*, *dlx3b* and *pax2a* otic expression in *hsy* mutant embryos demonstrates a defect in the initiation of otic placode induction and suggests that *foxi1* is the earliest-acting gene characterized thus far within the responding otic precursor domain.

Forkhead genes are known to function as transcriptional regulators (for a review, see Kaufmann and Knochel, 1996). Thus, it is possible that *foxi1* regulates the transcription of genes necessary for development of the otic placode in response to signals from surrounding tissues. However, we have shown that *foxi1* is also expressed in some mesendodermal cells underlying the presumptive otic anlagen of the ectodermal layer. Therefore, it is also possible that *foxi1* functions in a non-cell-autonomous manner to regulate otic development. In support of the first view we have demonstrated that misexpression of *foxi1* can induce ectopic *pax8* expression within the same cells. This observation, together with the loss of *pax8* otic expression in *hsy*, suggests a simple model in which *foxi1* would activate transcription of *pax8*. However, although it appears that *foxi1* is necessary, it is not sufficient for *pax8* otic expression, because not every cell that expresses *foxi1* also expresses *pax8* (Fig. 3). We also find that *pax8* is not expressed in every location where *foxi1* is ectopically expressed (Fig. 6). Therefore it appears that expression of *pax8* requires the function of regulatory factors in addition to *foxi1*.

Variability of the *hearsay* phenotype: multiple steps for otic placode induction

The loss of *pax8* expression observed in *hsy* embryos is a robust phenotype; expression of this gene was always absent in the presumptive otic domains of *hsy* mutant embryos. However, many *hsy* embryos develop an otic vesicle, albeit a small and malformed one. Thus, it appears that there is no absolute requirement for *foxi1* or *pax8* to form at least some aspects of an otic vesicle, nor is ectopic expression of these two genes sufficient to produce one.

Why this variability in otic placode and vesicle formation? One possibility is that another *foxi1*-like gene is present in the zebrafish genome. It has been suggested that ray-finned fish have undergone an additional round of genome duplication after diverging from the tetrapod lineage, and many gene families (Hox, Dlx, Msx, Eng) contain additional genes in the zebrafish genome (Postlethwait et al., 1998). If a second *foxi1* gene exists, it may be able to partially overcome the loss of the *foxi1*/*hsy* gene.

Another possibility arises from observations that embryonic induction of the otic placode occurs in multiple, overlapping steps (Baker and Bronner-Fraser, 2001; Torres and Giraldez, 1998). Recently, Groves and Bronner-Fraser have elegantly combined transplantation experiments with molecular analysis of otic placode induction (Groves and Bronner-Fraser, 2000). In chick, *Pax-2* is expressed in the presumptive otic placode at the four- to five-somite stage, followed by *Sox-3* at the six-somite stage, *BMP-7* at the seven-somite stage, and *Notch* at the nine- to ten-somite stage, a few hours before otic placodes become morphologically visible. When anterior, non-otic epiblast was grafted to the presumptive otic region of progressively older (11- to 21-somite stage) hosts, the grafted tissue formed an epithelial (otic) vesicle and often expressed *Sox-3* and *BMP-7*. However, older hosts rarely induced *Pax-2* expression, the earliest otic marker used, in the graft. Similarly, we observe later otic expression of markers such as *dlx3b*, *dlx5a* and *dlx4b* in the subset of *hsy* embryos that form a small otic vesicle, indicating that *foxi1* and/or *pax8* are not absolutely required for the expression of these genes. It has also been shown that signals for otic placode induction emanate from multiple tissues. For example, in zebrafish, heterotopic transplants of mesendoderm from early gastrula embryos can induce ectopic otic vesicles (Woo and Fraser, 1997). Mendonsa and Riley have used *one eyed pinhead* (*oep*) mutant and *notail* (*ntl*)/*oep* double mutant zebrafish embryos to show that genetic removal of mesendodermal cells leads to a severe delay in otic placode induction (Mendonsa and Riley, 1999). This delay is concomitant with a loss of *pax8* induction in the otic primordia (Phillips et al., 2001). Despite these defects, otic vesicles form, although they are variably smaller than wild type and lack one or both otoliths. Together, these observations demonstrate that otic vesicle formation can be uncoupled from the expression of early marker genes, and that a later source of otic vesicle-inducing signals can partially compensate for the loss of early

mesendodermal signaling. Thus, *foxi1*, like *pax8*, might only be transiently required in early otic primordia, and continued inductive influences can partially and variably bypass this requirement.

Induction of the otic placode

In zebrafish, *fgf3* and *fgf8* are expressed in both early mesendoderm and in the developing hindbrain during the stage when otic placode induction occurs, but not within the otic precursor tissues. These two genes play a redundant role in otic induction; inactivation of both *fgf3* and *fgf8* at the same time blocks otic placode induction and expression of *pax8* in the otic primordia (Phillips et al., 2001). Interestingly, some of these embryos still form a small otic vesicle, reminiscent of *hsy*.

Evidence from zebrafish and chick suggests that there are other factors in addition to *fgf3/8* involved in otic placode induction. In chick, *FGF19* is co-expressed with *FGF3* in paraxial cephalic mesoderm around the time of otic induction (Ladher et al., 2000), and transplants of mesoderm expressing *FGF19* to anterior ectoderm can induce expression of otic markers. Furthermore, *FGF19* requires the synergistic action of *Wnt8c*, which is induced by *FGF19* in overlying neural tissue. Although *fgf19* has not been reported in zebrafish, *fgf3* is expressed early in gastrulation in cephalic mesoderm, subjacent to the presumptive otic primordia (Phillips et al., 2001). Genetic removal of mesendodermal cells in *oep* mutant embryos (Schier et al., 1997) abolishes this *fgf3* domain and leads to a delay in otic placode induction (Mendonsa and Riley, 1999), but inactivation of *fgf3* in wild-type embryos does not produce a similar delay (Phillips et al., 2001). This suggests that mesendodermal signals in addition to *fgf3* are disrupted in *oep*.

foxi1 and jaw formation

In addition to otic abnormalities, *hsy* embryos also display a defect in jaw formation. Although all the cartilaginous elements of the jaw are present, the spacing is more compact, and this compression presumably leads to a reduction in size of the jaw. The cartilaginous elements arise from the branchial arches, which are formed through complex interactions between endoderm, mesoderm and neural crest cells that migrate to the arches from the hindbrain. In zebrafish, several mutations have been identified that lead to defects in inner ear and jaw formation (Malicki et al., 1996; Piotrowski et al., 1996; Whitfield et al., 1996), but this association is not well understood. Both defects may be the consequence of inappropriate hindbrain patterning, an example of which is seen in the *valentino* mutant, which disrupts a bZip transcription factor expressed in the hindbrain (Moens et al., 1998). However, morphological analysis and expression of hindbrain markers *krox20* (Fig. 8) and *fgf3/8* (not shown) show no indication of hindbrain defects in *hsy*, and cranial crest derivatives outside the jaw appear unaffected.

In an alternative model, the otic placode may provide positional cues for neural crest cell migration (Malicki et al., 1996). In particular, the preotic hyoid neural crest and the postotic vagal crest migrate in close apposition to the otic placode (Schilling and Kimmel, 1994), and misguided migration could be the result of otic placode defects. In support of this model, we find that the hyoid and postotic neural crest domains are positioned more closely to each other in *hsy* mutant embryos (Fig. 7C-F). However, we have previously shown that loss of *dlx3b* and *dlx4b* function blocks otic placode formation but has no detectable effect on the formation of the jaws (Solomon and Fritz, 2002).

In a third model, *foxi1* may play a direct role in the development of the branchial arches. We have shown that *foxi1* is expressed within the branchial arches, apparently within the pouches that separate the individual arches. It is possible that *foxi1* may regulate the expression of factors that control neural crest migration within the ectoderm. Another possibility is that *foxi1* may be required for the proper development of the pouches and that loss of *foxi1* function in *hsy* leads to a failure of the neural crest populations within the individual arches to become fully separated. In support of this, we have shown that expression domains of neural crest markers *dlx2a* and *crestin* are more closely spaced in *hsy* (Fig. 8). Incomplete separation of neural crest among the arches could lead to the fusion and closer spacing of the neural crest-derived jaw cartilages observed in the older mutant embryos (Fig. 8).

In the light of these results, it appears more probable that *foxi1* is required for branchial arch formation. In this context, *hsy* is reminiscent of the *van gogh* (*vgo*) mutation, which disrupts the segmentation of the pharyngeal pouches, leading to malformation of the jaw, and displays an inner ear defect, but does not affect hindbrain patterning (Piotrowski and Nusslein-Volhard, 2000; Whitfield et al., 1996).

Foxi I class genes

Foxi I class genes have been described in humans (Larsson et al., 1995; Pierrou et al., 1994), mouse (Hulander et al., 1998; Overdier et al., 1997), rat (Clevidence et al., 1993) and *Xenopus* (Lef et al., 1994; Lef et al., 1996). However, it is unclear whether zebrafish *foxi1* is orthologous to any one of these genes. The *Xenopus FoxI1c* (Lef et al., 1996), *FoxI1a* and *FoxI1b* genes (Lef et al., 1994) share the highest degree of sequence conservation with the zebrafish gene. The expression pattern of the two *Xenopus* pseudoallelic variants *FoxI1a/b* (*XFD-2, XFD-2′*) does not suggest functional similarity to zebrafish *foxi1*. Of the three *Xenopus* FoxI genes, *FoxI1c* (*XFD-10*) is most similar to *foxi1* in sequence. However, *Xenopus FoxI1c* was reported to be expressed in the neuroectoderm and somites but not in the otic placode, unlike the pattern for *foxi1* we report (Lef et al., 1996). A very recent report provides a more detailed description of *Xenopus FoxI1c* (Pohl et al., 2002), which suggests that this gene is expressed in preplacodal tissue and the branchial arches, similar to our observations for *foxi1*. Thus, it now appears probable that *Xenopus FoxI1c* represents the ortholog of zebrafish *foxi1*.

Functional analysis for a *foxi* paralogue has only been reported in mouse (Hulander et al., 1998). Mice homozygous for a targeted disruption of the *Fkh10* locus (*Foxi1* – Mouse Genome Informatics) exhibit circling behavior, poor swimming ability and abnormal reaching response as well as profound hearing impairment, demonstrating vestibular and cochlear dysfunction. In addition, these mice display malformations of the inner ear in that a large, irregular cavity replaces the cochlea and vestibulum. At 9.5 days post-coitus (dpc), *Fkh10* is expressed exclusively in the otic vesicle, the stage when the otic vesicle first forms by invagination. Mouse *Fkh10* is also expressed in the epithelium of renal distal convoluted tubules at 16.0 dpc (Overdier et al., 1997), however

no renal dysfunction has been observed in mutant mice (Hulander et al., 1998), and we have not examined expression of zebrafish *foxi1* at larval or adult stages. These observations suggest that Foxi1 genes in fish and mammals play a role in the development of the inner ear, but clear discrepancies exist between the mouse and fish Foxi1 genes. Most notably, zebrafish *foxi1* is expressed early in the otic primordia, but is no longer detectable in the otic placodes or otic vesicles, whereas mouse *Fkh10* is expressed at a later stage in the otic vesicle. In addition, *Fkh10* mutant mice do not show any craniofacial abnormalities, and, unlike the fish *foxi1* gene, the mouse gene is not expressed in the branchial arches at the otic vesicle stage. As branchial arch expression is shared by the related zebrafish *foxi1* and *Xenopus FoxI1c* genes, it is possible that as yet unexamined members of this subfamily may show expression in the arches during murine development.

Individuals affected by Treacher Collins Syndrome (TCS; MIM #154500) display a phenotype that includes inner ear defects and craniofacial malformations reminiscent of the *hsy* phenotype. In most cases, this syndrome is inherited in an autosomal dominant fashion, and the pathogenic mutation has been shown to lie within the *TCOF1* gene, which maps to 5q32 (The Treacher Collins Syndrome Collaborative Group, 1996; Edwards et al., 1997; Gladwin et al., 1996; Wise et al., 1997). However, individuals forming a subset of TCS patients appear to inherit the syndrome in a recessive fashion and do not carry any obvious defects in the *TCOF1* gene, even though haplotype analysis suggests that the genetic defect is linked closely to the *TCOF1* locus (Edwards et al., 1997). The human *FOXI1* (*FKHL10*) gene, which encodes a protein with 40% sequence identity to zebrafish Foxi1, has been localized to chromosome 5q34 (Larsson et al., 1995). Northern analysis with 16 adult and five fetal tissues demonstrated kidney-specific expression, but no otic tissues were analyzed (Pierrou et al., 1994). Based on our data, the nearby *FOXI1* gene is an intriguing candidate for this recessively inherited syndrome, and this should be easily testable.

We thank Dr D. Martinez for help with classification of the *foxi*1 gene, T. Schilling for helpful insight in the analysis of the pharyngeal arch defect and N. L'Hernault for generating sections of the *foxi1* in situ. We also thank S. L'Hernault and T. Piotrowski for their critical reading of the manuscript. A.F. was supported by a grant from NIDCD (R01-DC04701).

REFERENCES

Adamska, M., Herbrand, H., Adamski, M., Kruger, M., Braun, T. and Bober, E. (2001). FGFs control the patterning of the inner ear but are not able to induce the full ear program. *Mech. Dev.* **109**, 303-313.

Aitola, M., Carlsson, P., Mahlapuu, M., Enerback, S. and Pelto-Huikko, M. (2000). Forkhead transcription factor FoxF2 is expressed in mesodermal tissues involved in epithelio-mesenchymal interactions. *Dev. Dyn.* **218**, 136-149.

Akimenko, M. A., Ekker, M., Wegner, J., Lin, W. and Westerfield, M. (1994). Combinatorial expression of three zebrafish genes related to distal-less: part of a homeobox gene code for the head. *J. Neurosci.* **14**, 3475-3486.

Baker, C. V. and Bronner-Fraser, M. (2001). Vertebrate cranial placodes i. embryonic induction. *Dev. Biol.* **232**, 1-61.

Biggs, W. H., 3rd and Cavenee, W. K. (2001). Identification and characterization of members of the FKHR (FOX O) subclass of winged-helix transcription factors in the mouse. *Mamm. Genome* **12**, 416-425.

Boggetti, B., Argenton, F., Haffter, P., Bianchi, M. E., Cotelli, F. and Beltrame, M. (2000). Cloning and expression pattern of a zebrafish homolog of forkhead activin signal transducer (FAST), a transcription factor mediating Nodal-related signals. *Mech. Dev.* **99**, 187-190.

Chisaka, O., Musci, T. S. and Capecchi, M. R. (1992). Developmental defects of the ear, cranial nerves and hindbrain resulting from targeted disruption of the mouse homeobox gene *Hox-1.6*. *Nature* **355**, 516-520.

Clevidence, D. E., Overdier, D. G., Tao, W., Qian, X., Pani, L., Lai, E. and Costa, R. H. (1993). Identification of nine tissue-specific transcription factors of the hepatocyte nuclear factor 3/forkhead DNA-binding-domain family. *Proc. Natl. Acad. Sci. USA* **90**, 3948-3952.

Clevidence, D. E., Overdier, D. G., Peterson, R. S., Porcella, A., Ye, H., Paulson, K. E. and Costa, R. H. (1994). Members of the HNF-3/forkhead family of transcription factors exhibit distinct cellular expression patterns in lung and regulate the surfactant protein B promoter. *Dev. Biol.* **166**, 195-209.

Cordes, S. P. and Barsh, G. S. (1994). The mouse segmentation gene *kr* encodes a novel basic domain-leucine zipper transcription factor. *Cell* **79**, 1025-1034.

Dirksen, M. L. and Jamrich, M. (1995). Differential expression of fork head genes during early *Xenopus* and zebrafish development. *Dev. Genet.* **17**, 107-116.

Dou, C. L., Li, S. and Lai, E. (1999). Dual role of brain factor-1 in regulating growth and patterning of the cerebral hemispheres. *Cereb. Cortex* **9**, 543-550.

Edwards, S. J., Gladwin, A. J. and Dixon, M. J. (1997). The mutational spectrum in Treacher Collins Syndrome reveals a predominance of mutations that create a premature-termination codon. *Am. J. Hum. Genet.* **60**, 515-524.

Ekker, M., Akimenko, M. A., Bremiller, R. and Westerfield, M. (1992). Regional expression of three homeobox transcripts in the inner ear of zebrafish embryos. *Neuron* **9**, 27-35.

Ellies, D. L., Stock, D. W., Hatch, G., Giroux, G., Weiss, K. M. and Ekker, M. (1997). Relationship between the genomic organization and the overlapping embryonic expression patterns of the zebrafish dlx genes. *Genomics* **45**, 580-590.

Epstein, D. J., Vekemans, M. and Gros, P. (1991). Splotch (Sp2H), a mutation affecting development of the mouse neural tube, shows a deletion within the paired homeodomain of Pax-3. *Cell* **67**, 767-774.

Gladwin, A. J., Dixon, J., Loftus, S. K., Edwards, S., Wasmuth, J. J., Hennekam, R. C. and Dixon, M. J. (1996). Treacher Collins Syndrome may result from insertions, deletions or splicing mutations, which introduce a termination codon into the gene. *Hum. Mol. Genet.* **5**, 1533-1538.

Groves, A. K. and Bronner-Fraser, M. (2000). Competence, specification and commitment in otic placode induction. *Development* **127**, 3489-3499.

Hukriede, N., Fisher, D., Epstein, J., Joly, L., Tellis, P., Zhou, Y., Barbazuk, B., Cox, K., Fenton-Noriega, L., Hersey, C. et al. (2001). The LN54 radiation hybrid map of zebrafish expressed sequences. *Genome Res.* **11**, 2127-2132.

Hukriede, N. A., Joly, L., Tsang, M., Miles, J., Tellis, P., Epstein, J. A., Barbazuk, W. B., Li, F. N., Paw, B., Postlethwait, J. H. et al. (1999). Radiation hybrid mapping of the zebrafish genome. *Proc. Natl. Acad. Sci. USA* **96**, 9745-9750.

Hulander, M., Wurst, W., Carlsson, P. and Enerback, S. (1998). The winged helix transcription factor Fkh10 is required for normal development of the inner ear. *Nat. Genet.* **20**, 374-376.

Itoh, M., Kudoh, T., Dedekian, M., Kim, C. H. and Chitnis, A. B. (2002). A role for iro1 and iro7 in the establishment of an anteroposterior compartment of the ectoderm adjacent to the midbrain-hindbrain boundary. *Development* **129**, 2317-2327.

Jacobson, A. G. (1963). The determination and positioning of the nose, lens and ear. III. Effects of reversing the antero-posterior axis of epidermis, neural plate and neural fold. *J. Exp. Zool.* **154**, 285-291.

Jacobson, A. G. (1966). Inductive processes in embryonic development. *Science* **152**, 25-34.

Jowett, T. (2001). Double in situ hybridization techniques in zebrafish. *Methods* **23**, 345-358.

Kaufmann, E. and Knochel, W. (1996). Five years on the wings of fork head. *Mech. Dev.* **57**, 3-20.

Kimmel, C. B., Ballard, W. W., Kimmel, S. R., Ullmann, B. and Schilling, T. F. (1995). Stages of embryonic development of the zebrafish. *Dev. Dyn.* **203**, 253-310.

Kops, G. J. and Burgering, B. M. (1999). Forkhead transcription factors: new insights into protein kinase B (c-akt) signaling. *J. Mol. Med.* **77**, 656-665.

Kozlowski, D. J., Murakami, T., Ho, R. K. and Weinberg, E. S. (1997). Regional cell movement and tissue patterning in the zebrafish embryo revealed by fate mapping with caged fluorescein. *Biochem. Cell Biol.* **75**, 551-562.

Krauss, S., Johansen, T., Korzh, V. and Fjose, A. (1991). Expression of the zebrafish paired box gene pax[zf-b] during early neurogenesis. *Development* **113**, 1193-1206.

Kudoh, T., Tsang, M., Hukriede, N. A., Chen, X., Dedekian, M., Clarke, C. J., Kiang, A., Schultz, S., Epstein, J. A., Toyama, R. et al. (2001). A gene expression screen in zebrafish embryogenesis. *Genome Res.* **11**, 1979-1987.

Ladher, R. K., Anakwe, K. U., Gurney, A. L., Schoenwolf, G. C. and Francis-West, P. H. (2000). Identification of synergistic signals initiating inner ear development. *Science* **290**, 1965-1967.

Lai, E., Prezioso, V. R., Smith, E., Litvin, O., Costa, R. H. and Darnell, J. E., Jr (1990). HNF-3A, a hepatocyte-enriched transcription factor of novel structure is regulated transcriptionally. *Genes Dev.* **4**, 1427-1436.

Larsson, C., Hellqvist, M., Pierrou, S., White, I., Enerback, S. and Carlsson, P. (1995). Chromosomal localization of six human forkhead genes, freac-1 (FKHL5), -3 (FKHL7), -4 (FKHL8), -5 (FKHL9), -6 (FKHL10), and -8 (FKHL12). *Genomics* **30**, 464-469.

Lef, J., Clement, J. H., Oschwald, R., Koster, M. and Knochel, W. (1994). Spatial and temporal transcription patterns of the forkhead related XFD-2/XFD-2′ genes in *Xenopus laevis* embryos. *Mech. Dev.* **45**, 117-126.

Lef, J., Dege, P., Scheucher, M., Forsbach-Birk, V., Clement, J. H. and Knochel, W. (1996). A fork head related multigene family is transcribed in *Xenopus laevis* embryos. *Int. J. Dev. Biol.* **40**, 245-253.

Li, Y., Allende, M. L., Finkelstein, R. and Weinberg, E. S. (1994). Expression of two zebrafish orthodenticle-related genes in the embryonic brain. *Mech. Dev.* **48**, 229-244.

Lufkin, T., Dierich, A., LeMeur, M., Mark, M. and Chambon, P. (1991). Disruption of the *Hox-1.6* homeobox gene results in defects in a region corresponding to its rostral domain of expression. *Cell* **66**, 1105-1119.

Luo, R., An, M., Arduini, B. L. and Henion, P. D. (2001). Specific pan-neural crest expression of zebrafish Crestin throughout embryonic development. *Dev. Dyn.* **220**, 169-174.

Mahmood, R., Kiefer, P., Guthrie, S., Dickson, C. and Mason, I. (1995). Multiple roles for FGF-3 during cranial neural development in the chicken. *Development* **121**, 1399-1410.

Malicki, J., Schier, A. F., Solnica-Krezel, L., Stemple, D. L., Neuhauss, S. C., Stainier, D. Y., Abdelilah, S., Rangini, Z., Zwartkruis, F. and Driever, W. (1996). Mutations affecting development of the zebrafish ear. *Development* **123**, 275-283.

Mansouri, A., Chowdhury, K. and Gruss, P. (1998). Follicular cells of the thyroid gland require *Pax8* gene function. *Nat. Genet.* **19**, 87-90.

Mendonsa, E. S. and Riley, B. B. (1999). Genetic analysis of tissue interactions required for otic placode induction in the zebrafish. *Dev. Biol.* **206**, 100-112.

Miller, L. M., Gallegos, M. E., Morisseau, B. A. and Kim, S. K. (1993). lin-31, a *Caenorhabditis elegans* HNF-3/fork head transcription factor homolog, specifies three alternative cell fates in vulval development. *Genes Dev.* **7**, 933-947.

Moens, C. B., Cordes, S. P., Giorgianni, M. W., Barsh, G. S. and Kimmel, C. B. (1998). Equivalence in the genetic control of hindbrain segmentation in fish and mouse. *Development* **125**, 381-391.

Nasevicius, A. and Ekker, S. C. (2000). Effective targeted gene 'knockdown' in zebrafish. *Nat. Genet.* **26**, 216-220.

Odenthal, J. and Nusslein-Volhard, C. (1998). *fork head* domain genes in zebrafish. *Dev. Genes Evol.* **208**, 245-258.

Overdier, D. G., Ye, H., Peterson, R. S., Clevidence, D. E. and Costa, R. H. (1997). The winged helix transcriptional activator HFH-3 is expressed in the distal tubules of embryonic and adult mouse kidney. *J. Biol. Chem.* **272**, 13725-13730.

Oxtoby, E. and Jowett, T. (1993). Cloning of the zebrafish *krox-20* gene (*krx-20*) and its expression during hindbrain development. *Nucleic Acids Res.* **21**, 1087-1095.

Pfeffer, P. L., Gerster, T., Lun, K., Brand, M. and Busslinger, M. (1998). Characterization of three novel members of the zebrafish Pax2/5/8 family: dependency of Pax5 and Pax8 expression on the Pax2.1 (noi) function. *Development* **125**, 3063-3074.

Phillips, B. T., Bolding, K. and Riley, B. B. (2001). Zebrafish fgf3 and fgf8 encode redundant functions required for otic placode induction. *Dev. Biol.* **235**, 351-365.

Pierrou, S., Hellqvist, M., Samuelsson, L., Enerback, S. and Carlsson, P. (1994). Cloning and characterization of seven human forkhead proteins: binding site specificity and DNA bending. *EMBO J.* **13**, 5002-5012.

Piotrowski, T. and Nusslein-Volhard, C. (2000). The endoderm plays an important role in patterning the segmented pharyngeal region in zebrafish (*Danio rerio*). *Dev. Biol.* **225**, 339-356.

Piotrowski, T., Schilling, T. F., Brand, M., Jiang, Y. J., Heisenberg, C. P., Beuchle, D., Grandel, H., van Eeden, F. J., Furutani-Seiki, M., Granato, M. et al. (1996). Jaw and branchial arch mutants in zebrafish II: anterior arches and cartilage differentiation. *Development* **123**, 345-356.

Pogoda, H. M., Solnica-Krezel, L., Driever, W. and Meyer, D. (2000). The zebrafish forkhead transcription factor FoxH1/Fast1 is a modulator of nodal signaling required for organizer formation. *Curr. Biol.* **10**, 1041-1049.

Pohl, B. S., Knochel, S., Dillinger, K. and Knochel, W. (2002). Sequence and expression of FoxB2 (XFD-5) and FoxI1c (XFD-10) in *Xenopus* embryogenesis. *Mech. Dev.* **117**, 283-287.

Postlethwait, J. H., Yan, Y. L., Gates, M. A., Horne, S., Amores, A., Brownlie, A., Donovan, A., Egan, E. S., Force, A., Gong, Z. et al. (1998). Vertebrate genome evolution and the zebrafish gene map. *Nat. Genet.* **18**, 345-349.

Represa, J., Leon, Y., Miner, C. and Giraldez, F. (1991). The int-2 proto-oncogene is responsible for induction of the inner ear. *Nature* **353**, 561-563.

Rubinstein, A. L., Lee, D., Luo, R., Henion, P. D. and Halpern, M. E. (2000). Genes dependent on zebrafish cyclops function identified by AFLP differential gene expression screen. *Genesis* **26**, 86-97.

Schier, A. F., Neuhauss, S. C., Helde, K. A., Talbot, W. S. and Driever, W. (1997). The *one-eyed pinhead* gene functions in mesoderm and endoderm formation in zebrafish and interacts with no tail. *Development* **124**, 327-342.

Schilling, T. F. and Kimmel, C. B. (1994). Segment and cell type lineage restrictions during pharyngeal arch development in the zebrafish embryo. *Development* **120**, 483-494.

Shimoda, N., Knapik, E. W., Ziniti, J., Sim, C., Yamada, E., Kaplan, S., Jackson, D., de Sauvage, F., Jacob, H. and Fishman, M. C. (1999). Zebrafish genetic map with 2000 microsatellite markers. *Genomics* **58**, 219-232.

Solomon, K. S. and Fritz, A. (2002). Concerted action of two dlx paralogs in sensory placode formation. *Development* **129**, 3127-3136.

Strahle, U., Blader, P., Henrique, D. and Ingham, P. W. (1993). *Axial*, a zebrafish gene expressed along the developing body axis, shows altered expression in cyclops mutant embryos. *Genes Dev.* **7**, 1436-1446.

The Treacher Collins Syndrome Collaborative Group (1996). Positional cloning of a gene involved in the pathogenesis of Treacher Collins Syndrome. *Nat. Genet.* **12**, 130-136.

Thisse, C. and Thisse, B. (1998). High resolution whole-mount in situ hybridization. *The Zebrafish Science Monitor* **5**, 8-9.

Topczewska, J. M., Topczewski, J., Solnica-Krezel, L. and Hogan, B. L. (2001). Sequence and expression of zebrafish *foxc1a* and *foxc1b*, encoding conserved forkhead/winged helix transcription factors. *Mech. Dev.* **100**, 343-347.

Toresson, H., Martinez-Barbera, J. P., Bardsley, A., Caubit, X. and Krauss, S. (1998). Conservation of BF-1 expression in amphioxus and zebrafish suggests evolutionary ancestry of anterior cell types that contribute to the vertebrate telencephalon. *Dev. Genes Evol.* **208**, 431-439.

Torres, M. and Giraldez, F. (1998). The development of the vertebrate inner ear. *Mech. Dev.* **71**, 5-21.

Vendrell, V., Carnicero, E., Giraldez, F., Alonso, M. T. and Schimmang, T. (2000). Induction of inner ear fate by FGF3. *Development* **127**, 2011-2019.

Waddington, C. H. (1937). The determination of the auditory placode in the chick. *J. Exp. Biol.* **14**, 232-239.

Weigel, D., Jurgens, G., Kuttner, F., Seifert, E. and Jackle, H. (1989). The homeotic gene fork head encodes a nuclear protein and is expressed in the terminal regions of the *Drosophila* embryo. *Cell* **57**, 645-658.

Westerfield, M. (2000). *The Zebrafish Book: A Guide for the Laboratory Use of Zebrafish (*Danio rerio*)*. Eugene, OR: University of Oregon Press.

Whitfield, T. T., Granato, M., van Eeden, F. J., Schach, U., Brand, M., Furutani-Seiki, M., Haffter, P., Hammerschmidt, M., Heisenberg, C. P., Jiang, Y. J. et al. (1996). Mutations affecting development of the zebrafish inner ear and lateral line. *Development* **123**, 241-254.

Wise, C. A., Chiang, L. C., Paznekas, W. A., Sharma, M., Musy, M. M., Ashley, J. A., Lovett, M. and Jabs, E. W. (1997). *TCOF1* gene encodes a putative nucleolar phosphoprotein that exhibits mutations in Treacher Collins Syndrome throughout its coding region. *Proc. Natl. Acad. Sci. USA* **94**, 3110-3115.

Woo, K. and Fraser, S. E. (1997). Specification of the zebrafish nervous system by nonaxial signals. *Science* **277**, 254-257.
Xu, P. X., Adams, J., Peters, H., Brown, M. C., Heaney, S. and Maas, R. (1999). Eya1-deficient mice lack ears and kidneys and show abnormal apoptosis of organ primordia. *Nat. Genet.* **23**, 113-117.
Xuan, S., Baptista, C. A., Balas, G., Tao, W., Soares, V. C. and Lai, E. (1995). Winged helix transcription factor BF-1 is essential for the development of the cerebral hemispheres. *Neuron* **14**, 1141-1152.
Yntema, C. L. (1933). Experiments on the determination of the ear ectoderm in the embryo of *amblyostoma punctatum*. *J. Exp. Zool.* **65**, 317-357.
Yntema, C. L. (1950). An induction of the ear from foreign ectoderm in the salamander. *J. Exp. Zool.* **113**, 211-244.